

**Nenad Mitrovic**

Research Associate  
University of Belgrade  
Innovation Center of Faculty of Mechanical  
Engineering

**Milos Milosevic**

Research Associate  
University of Belgrade  
Innovation Center of Faculty of Mechanical  
Engineering

**Aleksandar Sedmak**

Professor  
University of Belgrade  
Faculty of Mechanical Engineering

**Aleksandar Petrovic**

Professor  
University of Belgrade  
Faculty of Mechanical Engineering

**Radica Prokic-Cvetkovic**

Professor  
University of Belgrade  
Faculty of Mechanical Engineering

# Application and Mode of Operation of Non-Contact Stereometric Measuring System of Biomaterials

*New optical stereometric methods are becoming commonplace in investigations of mechanical behaviour of biomaterials. An understanding of the mechanical behaviour of hard and soft tissues is of great importance in the design and investigation of biomaterials. The mechanical behaviour of biomaterials can be evaluated using a number of methods that are based on either contact or non-contact schemes for displacement measurement. The method for full-field measurement of strain is done by using the ARAMIS three-dimensional image correlation system. The system uses two digital cameras that provide a synchronized stereo view of the specimen and the results show the complete strain field during the tests. Several examples are presented that highlight the use of stereometric measuring system for modern biomaterials. It is shown that this measuring methodology can capture the trends of the experiments.*

**Keywords:** stereometric method, biomaterials, strain measurement.

## 1. INTRODUCTION

New, advanced biomaterials place huge challenges on the existing measurement technologies for determining the mechanical properties of these materials, as well as just measuring the full-field displacement and strain of these materials.

3D measurement results are always required as 3D object shows non-linear deformation behaviour. Measuring systems for 3D deformation analyses provide the right tools for understanding of biomaterials and components as they are independent of material, size and geometry. 3D analysis of surface deformations, e.g. vibrational spectroscopy [1], real time holographic technique [2], can lead to better understanding of mechanical properties of biomaterials, and complement other contemporary means of analysis. Measuring systems consider the real component geometry which would not be possible with traditional measuring devices, such as strain gauges, displacement sensors (LVDT), vibrometers, etc.

More techniques and holographic interferometry (ESPI) from theoretical perspective [3] have been thoroughly described as well as the application engineering viewpoint [4].

A system for 3D optical deformation measurement is presented, alongside with basic instructions for system settings, measurement procedures and result processing. Some of the application possibilities are also presented for different kinds of biomaterials and real objects (components, parts, etc.).

## 2. OPTICAL DEFORMATION MEASUREMENT SYSTEM

---

Received: January 2011, Accepted: May 2011  
Correspondence to: Milos Milosevic  
Innovation Center of Faculty of Mechanical Engineering,  
Kraljice Marije 16, 11120 Belgrade 35, Serbia  
E-mail: mmilosevic@mas.bg.ac.rs

The optical deformation measurement system consists of special sets of stereo cameras and lenses, and Aramis software [5]. The system uses two digital cameras that provide a synchronized stereo view of the specimen or object (Fig. 1). The system also includes a stand, providing the stability of the sensors, a power control and image recording unit, as well as the data processing system, as shown in Figure 1.

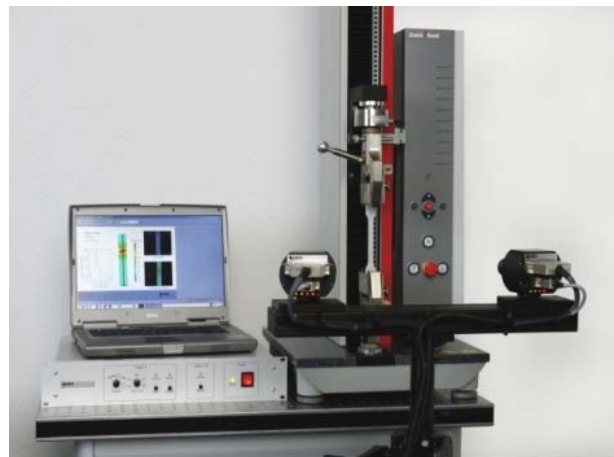


Figure 1. Hardware, software and specimen

### 2.1 System application

The system is applied in solving problems when analyzing structure integrity, determining properties of materials, verifying and refining numerical calculations [6,7], etc. It is suitable for analysis of irregular object geometries made of various materials, such as metal, composite, gum, wood, organic materials, biomaterials, and for analysis of hyper-elastic materials [6-9].

Aramis delivers complete 3D surface, displacement and strain results, where a large number of traditional measuring devices are required (strain gauges, LVDTs extensometers). This software provides all results for

static and dynamic tests even at high speeds for smallest to largest components for:

- Strength assessment;
- Vibration analysis;
- Durability studies;
- Crash tests.

Aramis is a non-contact and material independent measuring system providing, for static or dynamically loaded test objects, accurate:

- 3D surface coordinates;
- 3D displacements and velocities;
- Surface strain values (major and minor strain, thickness reduction);
- Strain rates.

Aramis helps to better understand material and component behaviour and is well suited to monitor experiments with high temporal and local resolution. Aramis is used for:

- Determination of biomaterial properties (R- and N-values, FLC, Young's Modulus, etc.);
- Component analysis (crash tests, vibration analysis, durability studies, etc.);
- Verification of Finite Element (FE) Analysis.

## 2.2 Verification of FE simulations

As part of complex process chains, optical measuring systems have become important tools in industrial processes in the last years. Together with the numerical simulation they have significant potential for quality improvement and optimization of development time for products and production. The 3D measuring systems can link to the component's original 3D CAD data for transformations, direct comparisons and visualizations [5].

Aramis supports the full-field verification of FE-simulations. Determining material parameters with Aramis helps to evaluate and improve the existing material models. The import of FE result datasets allows performing numerical full-field comparisons to FE simulations for all kinds of component tests.

## 2.3 Real-time data processing

The Aramis software provides real-time results for multiple measurement positions from the test objects surface, which can replace polarimetric optical fibre sensors for stress-strain monitoring [10]. These are directly transferred to testing devices, data acquisition units or processing software (e.g. Lab View, DIAdem, MS Excel, etc.) and are used for:

- Control of testing devices;
- Long-term tests with smallest storage requirements;
- Vibration analysis;
- 3D Video extensometer.

## 3. MODE OF OPERATION

With optical measurement techniques, the coordinates, displacements and strains will be determined only on the surface of objects. This means, that the calculation is limited to local strains, which are tangential to the surface [11].

As additional information perpendicular to the surface is missing, it is not possible to calculate a complete 3D strain tensor (strain values). In this case, the calculation of the thickness change is based on the assumption of volume constancy of the material during loading [12].

Regarding a unit square in the 2D space (points (0/0), (0/1), (1/0), (1/1)) the deformation introduced by this stretch tensor is shown in Figure 2.

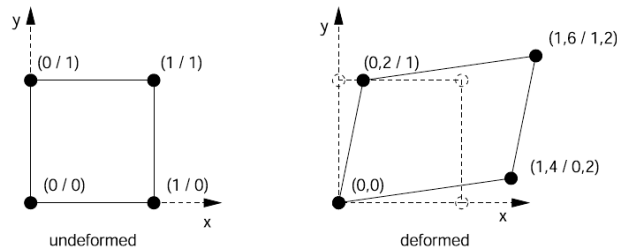


Figure 2. Example for the deformation of a unit square

For the geometrical interpretation of the value  $\epsilon_{xy}$  the shear angle  $\gamma_{xy}$  is used. This angle describes the change of the 90° angle in the undeformed state to a new angle in the deformed state, as shown in Figure 3.

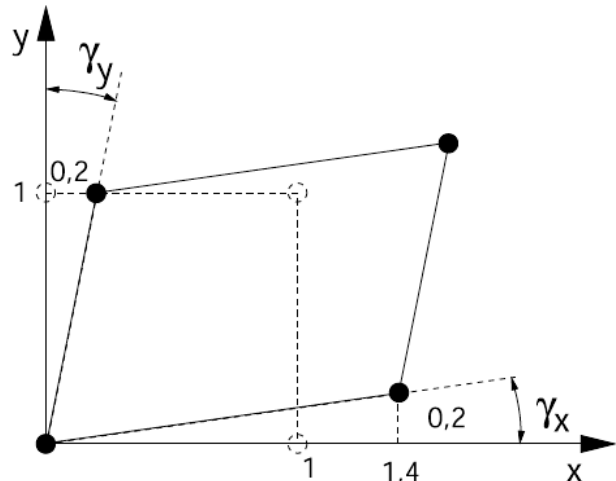


Figure 3. Shear angle definition

The fixed values for  $\gamma_x$  and  $\gamma_y$  show that the orientation of the parallelogram to the coordinate system is fixed. The stretch tensor cannot describe rotations. This coordinate system is defined as  $x''-y''$  system.

### 3.1 Definition of the 2D coordinate system and strain directions

The deformation gradient tensor  $\mathbf{F}$  creates a functional connection of the coordinates of the deformed points  $P_{v,i}$  with the coordinates of the undeformed points  $P_{u,i}$  ( $i$  being the index for the different points). The functional connection for each local point is as follows:

$$P_{v,I} = u_i + F \cdot P_{u,I} \quad (1)$$

with:  $P_{v,I}$  – coordinates of the undeformed point,  $P_{u,I}$  – coordinates of the deformed point,  $u_i$  – rigid body translation.

The deformation gradient tensor  $\mathbf{F} = \mathbf{R} \cdot \mathbf{U}$  can be split to the rotation matrix  $\mathbf{R}$  and the stretch tensor  $\mathbf{U}$ . The rotation matrix  $\mathbf{R}$  describes the rotation of the points and the directions, as shown in Figure 4.

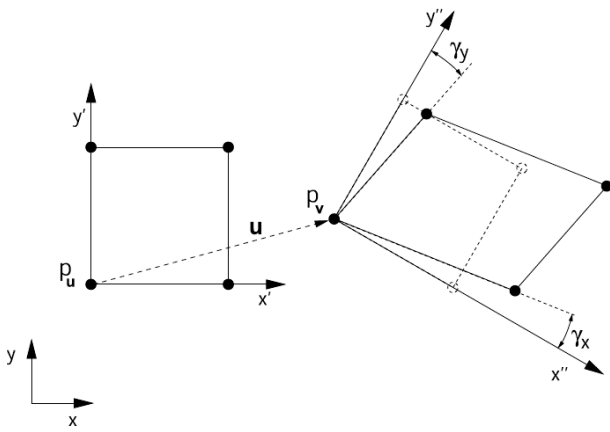


**Figure 4: Definition of the coordinate systems (based on the deformation of a unit square)**

This context is shown in Figure 4. Different coordinate systems are used:

- $x$ - $y$ : global coordinate system;
- $x'$ - $y'$ : local undeformed coordinate system;
- $x''$ - $y''$ : local deformed coordinate system = directions of strain.

The coordinates of the point (e.g.  $p_u$  and  $p_v$ ) are calculated in the global  $x$ - $y$  coordinate system. For the 2D discussion, the coordinate system  $x'$ - $y'$  is parallel to  $x$ - $y$ , but it is placed in the undeformed position of the point of interest  $P_{u,i}$ .

### 3.2 Major and minor strain derived from the deformation gradient tensor

The disadvantage for  $\epsilon_x$  and  $\epsilon_y$  to be defined as dependent on the coordinate system can be eliminated by calculating major and minor strain values. The symmetrical matrix  $\mathbf{U}$  can be transformed to the main diagonal form. The two eigenvalues  $\lambda_1$  and  $\lambda_2$  can be calculated as follows (2):

$$\lambda_{1,2} = 1 + \frac{\epsilon_x + \epsilon_y}{2} \pm \sqrt{\left(\frac{\epsilon_x + \epsilon_y}{2}\right)^2 - (\epsilon_x \cdot \epsilon_y - \epsilon_{x,y}^2)} \quad (2)$$

Depending on the choice of the strain measure, the stretch ratios  $\lambda_1$  and  $\lambda_2$  can be transformed into corresponding strain values. Based on the larger eigenvalue the major strain is determined ( $\epsilon_1$  or  $\phi_1$ ) and based on the smaller eigenvalue the minor strain ( $\epsilon_2$  or  $\phi_2$ ). The corresponding eigenvectors determine the two directions of major and minor strain. The strain values thus determined are independent of the coordinate system and are universally applicable.

The effective strain according to von Mises results from the (3):

$$\phi_V = \sqrt{\frac{2}{3}(\phi_1^2 + \phi_2^2 + \phi_3^2)} \quad (3)$$

As  $\phi_3$  is included in (3), the effective strain is only valid if the volume constancy is valid.

The effective strain according to von Tresca results from the (4):

$$\phi_V = |\phi|_{\max} \quad (4)$$

### 3.3 Definition of the $x$ - $y$ strain values and the strain directions in 3D

To be able to use the above defined 2D models of calculation, an extended definition for the local directions is needed. The local strain coordinate systems must be tangential to the local surface and for the strain calculation the 3D data must be transformed into 2D space.

In Figure 5 the definition of the local strain directions is shown. The global coordinate system  $x$ - $y$ - $z$  cannot be used, in general, for the local strain values. The  $x$ - $y$ - $z$  coordinate system, in general, is not parallel to the local tangential directions. For the local strain calculation in ARAMIS an  $x'$ - $y'$  coordinate system is defined for the undeformed state as follows.

For each point (e.g. the point P1 in Figure 5.):

- the local strain direction  $x'$  is:
  - tangential to the surface of the local point;
  - parallel to the  $x$ - $z$  plane;
- the local direction  $y'$  is:
  - tangential to the surface of the local point;
  - perpendicular to the local  $x'$ .

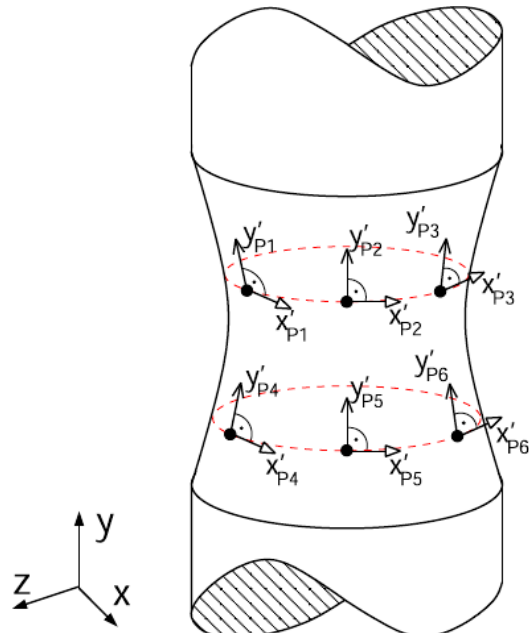


**Figure 5. Definition of the undeformed local surface strain coordinate system in 3D**

In general, both directions ( $x'$  and  $y'$ ) are not parallel to the global coordinate system. This is shown in Figure 6. In the deformed state the  $x''$ - $y''$  strain directions are still tangential to the surface in the local 3D points and are defined by the stretch tensor in the same way as in the 2D situation.

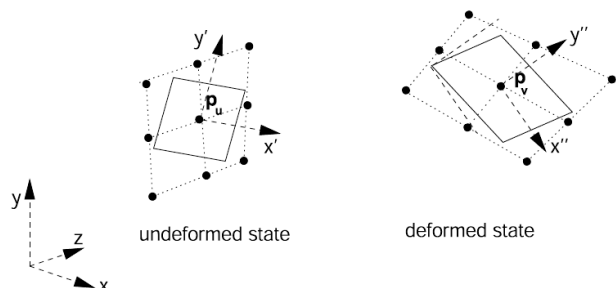


**Figure 6. Definition of the local surface strain coordinate system in 3D**

The unit square is deformed to a parallelogram. The geometry of the parallelogram together with the stretch tensor ( $\gamma_x$  and  $\gamma_y$ ) define the local strain directions ( $x''$  and  $y''$ ) in the deformed state, as shown in Figure 6.

Parallel to the definition of the directions the 3D data must be transformed into the 2D space. Two different models can be used. These models are based on planes or splines.

### 3.4 The plane model

The first model assumes that the local neighbourhood of a point can be well approximated by a tangential plane. Due to the arbitrary deformation of the surface, the tangential plane needs to be calculated separately for the deformed and undeformed state. The points in the local neighbourhood are then projected perpendicularly onto the tangential plane. The result is two sets of points, for the deformed and undeformed state, in the two-dimensional space in which the strain now can be calculated. Summarized, this process consists of the following tasks:

- Calculation of the tangential plane;
- Transformation of the 3D neighbourhoods into the tangential planes;
- Coordinate transformation of the tangential plane into the 2D space ( $x'-y'$  and  $x''-y''$  coordinate system);
- Calculation of the deformation gradient tensor from the 2D sets of points.

### 3.5 The spline model

The tangential model described above provides good results as long as the assumption of the linearization of a local neighbourhood of points is valid. In deep drawing, the deformed materials have in part strong locally curved planes. The problem now is to apply the characteristics to be measured to the respective object in such a frequency that the assumption of local linearity is still given. However, this characteristic can hardly be provided in reality. Therefore, it is better to use other models which are more accurate in modelling the true shape of the surface. Splines are a good model for continuously curved lines.

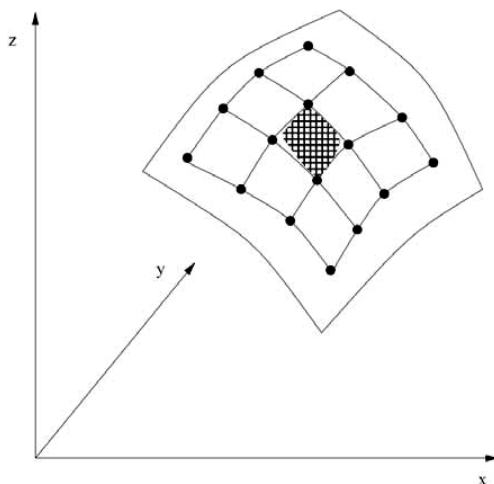


Figure 7. Four-sided facet with adjacent points

In order to calculate the side length not only according to a linear model, it is necessary to have more

information than two points on a side. This means that the adjacent points of a four-sided facet have to be included in the calculations. Adjacent points of the hatched four-sided facet are shown in Figure 7.

In the facet, the side lengths are calculated using the formed splines. The resulting lengths can be used to construct a quadrangle in the two-dimensional space. Now, the strain calculations described above can be used.

## 4. MEASUREMENT PROCESS

### 4.1 System calibration and preparation of the measured object

Prior to starting the experiment, a system calibration must be performed. The calibration is performed by using the calibration panels or cross (Fig. 8), depending on the chosen measurement volume. This volume is chosen based on the dimensions of the measured object and all other dimensions are set based on it, in accordance with the tables in the instruction manual [13]. If the measurement volume and the camera position are successfully aligned by the calibration, the measurement may commence. Recalibration of the sensors is needed if the distance to object, angle between the cameras and camera lens alignment must be changed due to a different measurement volume. For correct calibration, the calibration deviation is 0.01 to 0.04 pixels.

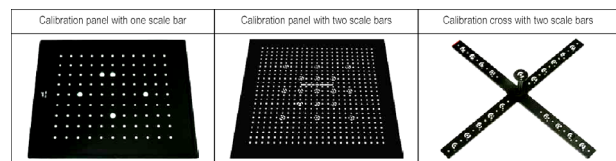


Figure 8. Calibration panels and cross [13]

The preparation of the object to be measured starts with the placement of referral points – markers. The referral points, in case of the Aramis system, are placed with black and/or white spray, in order to create the best possible contrast, and enable the software to track the changes occurring in the object as it undergoes the loading. Good and bad pattern are shown in Figure 9.

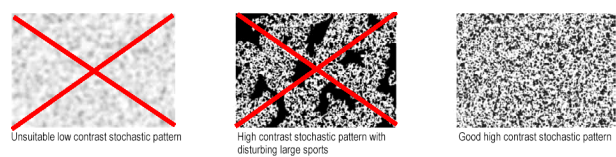


Figure 9. Examples of good and bad stochastic patterns [13]

### 4.2 Measurement procedure

After the successful calibration of the system and the measured object, the measurement procedure can start. The measurement includes creating a new project, setting the recording speed and lighting around the object. After creating the measuring project in the software, images are recorded in various load stages of the object. After the evaluating area is defined and a start point is determined, the measuring project is computed. During computation, Aramis observes the deformation of the object through the images by means of various square or rectangular image details (facets). Aramis

recognizes the surface structure of the measuring object in digital camera images and allocates coordinates to the image pixels. The first image in this measuring project represents the undeformed state of the object.

### 4.3 Result analysis

After the computation, result processing and preparation

for the final report is performed. Software tools enable subsequent data processing, such as data filtering or interpolation, if needed. To represent the results in diagrams, different types of primitives can be formed inside each state (part of a plane, part of a circle, curved part), or inside the whole object. An example of a (cylindrical) primitive and its application in result processing is given in the Figures 10 and 11.

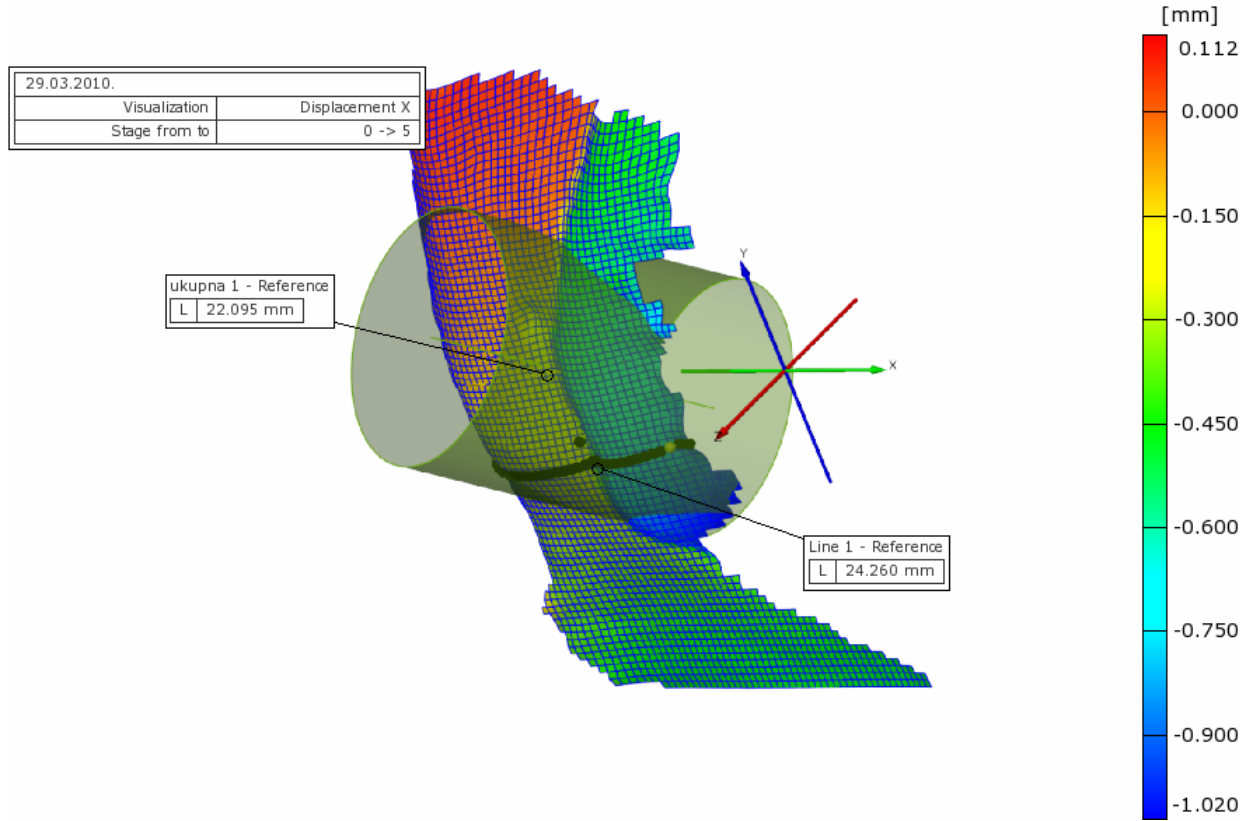


Figure 10. Cylindrical primitive

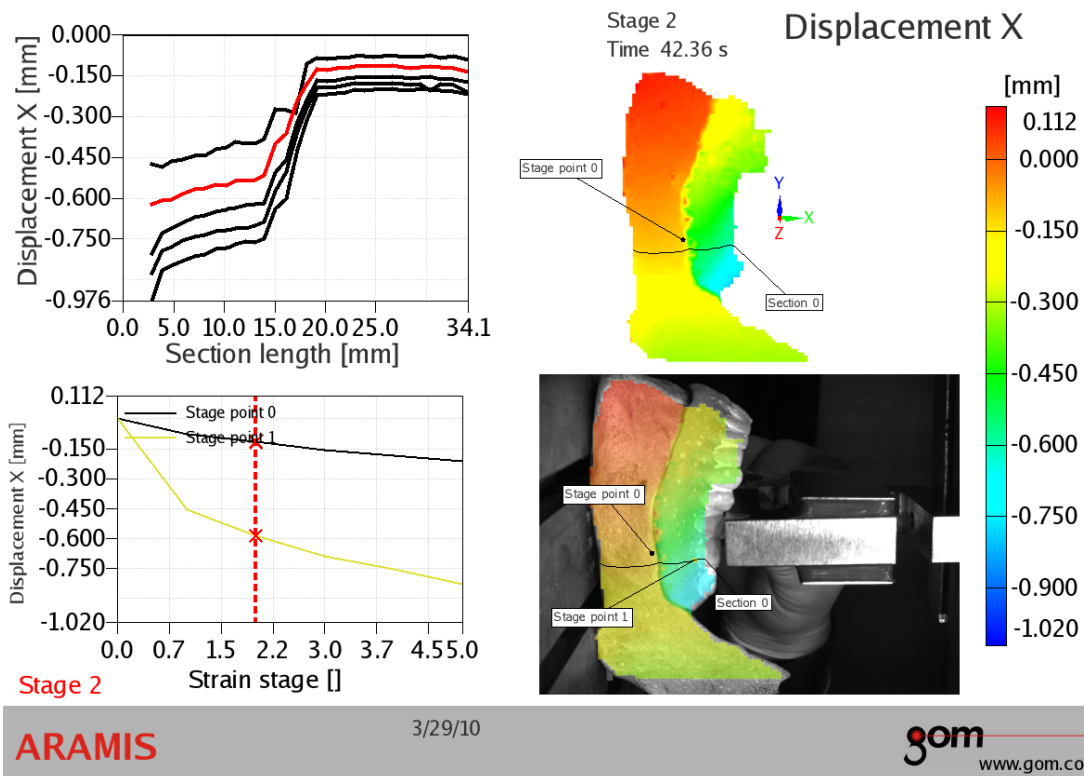


Figure 11. Example of an Aramis' report

## 5. CONCLUSION

The 3D optical strain and displacement analysis using digital image correlation represents a useful experimental approach that helps to better understand full displacement/strain fields of loaded biomaterials and biomaterial structures. Accurate software calculations, data post-processing with great number of options, and custom result presentation in reports, the possibilities of applying this method into current biomaterial studies are increased.

## REFERENCES

- [1] Paluszkiwicz, C., Kwiatek, W.M., Długoń, E., Weselucha-Birczyńska, A. and Piccinini, M.: Surface study of selected biomaterials using vibrational spectroscopy, *Acta Physica Polonica A*, Vol. 115, No. 2, pp. 533-536, 2009.
- [2] Pantelić, D., Blažić, L., Savić-Šević, S., Murić, B., Vasiljević, D., Panić, B. and Belić, I.: Holographic measurement of dental tissue contraction and stress, due to postpolymerization reaction, *Acta Physica Polonica A*, Vol. 112, No. 5, pp. 1157-1160, 2007.
- [3] Cloud, G.: *Optical Methods of Engineering Analysis*, Cambridge University Press, Cambridge 1998.
- [4] Tyson II, J.: Noncontact full-field strain measurement with 3D ESPI, *Sensors*, Vol. 17, No. 5, pp. 62-70, 2000.
- [5] GOM – Gesellschaft für Optische Messtechnik mbH, <http://www.gom.com>
- [6] Ahn, B. and Kim, J.: Measurement and characterization of soft tissue behavior with surface deformation and force response under large deformations, *Medical Image Analysis*, Vol. 14, No. 2, pp. 138-148, 2010.
- [7] Gilat, A., Schmidt, T. and Tyson, J.: Full field strain measurement during a tensile split Hopkinson bar experiment, *Journal de Physique IV*, Vol. 134, No. 1, pp. 687-692, 2006.
- [8] Hogström, P., Ringsberg, J.W. and Johnson, E.: An experimental and numerical study of the effects of length scale and strain state on the necking and fracture behaviours in sheet metals, *International Journal of Impact Engineering*, Vol. 36, No. 10-11, pp. 1194-1203, 2009.

- [9] Li, J., Fok, A.S.L., Satterthwaite, J. and Watts, D.C.: Measurement of the full-field polymerization shrinkage and depth of cure of dental composites using digital image correlation, *Dental Materials*, Vol. 25, No. 5, pp. 582-588, 2009.
- [10] Domanski, A.W., Lesiak, P., Milenko, K., Budaszewski, D., Chychlowski, M., Ertman, S., Tefelska, M., Wolinski, T.R., Jedrzejewski, K., Lewandowski, L., Jasiewicz, W., Helsztynski, J. and Boczkowska, A.: Comparison of bragg and polarimetric optical fiber sensors for stress monitoring in composite materials, *Acta Physica Polonica A*, Vol. 116, No. 3, pp. 294-297, 2009.
- [11] Kalpakjian, S. and Schmid, S.: *Manufacturing Engineering and Technology*, Pearson Education, Upper Saddle River, 2006.
- [12] Dieter, G.E.: *Mechanical Metallurgy*, McGraw-Hill, New York, 1988.
- [13] <https://support.gom.com>

---

### ПРИМЕНА И НАЧИН РАДА БЕЗКОНТАКТНОГ СИСТЕМА ЗА МЕРЕЊЕ ДЕФОРМАЦИЈА У ОБЛАСТИ БИОМАТЕРИЈАЛА

**Ненад Митровић, Милош Милошевић,  
Александар Седмак, Александар Петровић,  
Радица Прокић-Цветковић**

Нове оптичке стереометријске методе постају уобичајене у праћењу механичких карактеристика биоматеријала. Разумевање механичких карактеристика тврдих и меких ткива је од велике важности у дизајнирању и испитивању биоматеријала. Механичко понашање биоматеријала се може проценити коришћењем бројних метода које су засноване на контактном или безконтактном мерењу деформација. Мерење деформационог поља је у овом раду извршено помоћу система за тродимензионално мерење деформација и софтвера Арамис. Систем користи две дигиталне камере које омогућавају стерео приказ узорка, а у резултатима се добија комплетно деформационо поље. Приказано је неколико примера који истичу коришћење система у области биоматеријала и показано је да ова метода мерења може да испрати нове трендове експеримената.